Environmental and Sustainability Indicators 30 (2026) 101263

Contents lists available at ScienceDirect

Environmental and Sustainability Indicators

journal homepage: www.sciencedirect.com/journal/environmental-and-sustainability-indicators

Projecting the potential distribution of *Setaria palmifolia* in China in response to climate change

Yangzhou Xiang [a], Suhang Li [a], Ying Liu [b], Qiong Yang [a], Jinxin Zhang [c,d,*], Bin Yao [c,**], Yuan Li [e,***]

[a] School of Geography and Resources, Guizhou Education University, Guiyang, 550018, China
[b] School of Biological Sciences, Guizhou Education University, Guiyang, 550018, China
[c] Institute of Ecological Conservation and Restoration, Chinese Academy of Forestry, Beijing, 100091, China
[d] Grassland Research Center, National Forestry and Grassland Administration, Beijing, 100091, China
[e] Grasslands and Sustainable Farming, Production Systems Unit, Natural Resources Institute Finland, Halolantie 31A, Maaninka, FI−71750, Finland

ARTICLE INFO

Keywords:
Setaria palmifolia
MaxEnt model
Climate change
Model optimization
Introduction planning

ABSTRACT

Accurately predicting the potential distribution of *Setaria palmifolia* in China is crucial for assessing its climatic adaptability as a forage resource and for developing sustainable utilization strategies. This study systematically integrated 927 species distribution records while employing a comprehensive set of multidimensional environmental variables, including climate, topography, vegetation, and human activity. Using an optimized Maximum Entropy (MaxEnt) model, we simulated the potential geographic distribution of *S. palmifolia* under both current conditions and future scenarios (2050s, 2070s, 2090s) across three Shared Socioeconomic Pathways (SSP126, SSP370, SSP585). The results identified the key environmental factors influencing its distribution: precipitation of the warmest quarter, precipitation of the coldest quarter, and temperature diurnal range. These factors collectively contributed 93.4% to the model. Under current climatic conditions, the total potentially suitable habitat for *S. palmifolia* is approximately 177.22×10^4 km^2, primarily concentrated in southern China. Future projections indicate that the total suitable area will remain relatively stable across all scenarios (ranging from 177.22×10^4 to 196.80×10^4 km^2). However, its internal structure will undergo significant reorganization, with highly suitable habitat expanding from 12.20×10^4 km^2 (current) to between 29.69×10^4 and 50.39×10^4 km^2 depending on emission scenarios. By the 2070s, this expansion is projected to reach 35.80×10^4 to 50.39×10^4 km^2. Meanwhile, the distribution centroid shows complex, non-linear migration trajectories. This internal suitability reorganization pattern suggests that *S. palmifolia* responds to climate change through local adaptation rather than simple range shifts. Our findings provide critical scientific evidence and spatial decision-support for regional introduction planning, priority conservation area identification, and climate change adaptive management of *S. palmifolia* as a forage resource.

1. Introduction

As global climate change intensifies, agricultural ecosystems and the production they support are facing unprecedented challenges and opportunities (Yang et al., 2024). Rising temperatures, shifting precipitation patterns, and the increasing frequency of extreme climate events are profoundly affecting the geographical distribution and ecological adaptability of crops (Lesk et al., 2016, 2022). In this context, scientifically assessing and rationally utilizing plant resources with strong environmental adaptability has become a vital pathway for ensuring sustainable agricultural development and ecological security (Yang and Solangi, 2024).

Herbaceous plants, as key components of ecosystems, not only help maintain biodiversity but also hold significant economic value (Chen et al., 2025; Clemente-Villalba et al., 2023; Deng et al., 2022). In particular, herb species that combine ecological resilience with economic potential are of strategic importance for optimizing agricultural structures and promoting agroecological development through scientific

* Corresponding author. Institute of Ecological Conservation and Restoration, Chinese Academy of Forestry, Beijing, 100091, China.
** Corresponding author.
*** Corresponding author.
E-mail addresses: zhangjinxin@caf.ac.cn (J. Zhang), acmn21@caf.ac.cn (B. Yao), yuan.li@luke.fi (Y. Li).

https://doi.org/10.1016/j.indic.2026.101263
Received 4 December 2025; Received in revised form 9 April 2026; Accepted 10 April 2026
Available online 11 April 2026

introduction and cultivation (Nan, 2005; Tian et al., 2021). Species distribution models (SDMs) serve as essential tools in ecological research, enabling effective prediction of species' potential geographic ranges and offering key scientific support for the planned introduction and regional management of plant resources (Franklin, 2023). Among these, the Maximum Entropy (MaxEnt) model has been widely adopted to assess species' ecological responses to climate change, owing to its reliable performance and high predictive accuracy even with limited data (Phillips and Dudík, 2008). It has shown great promise in guiding targeted introduction of forage and resource plants (Capera-Aragones et al., 2023; Tatian et al., 2025), thereby acting as a critical bridge between foundational research and practical application.

To date, while some progress has been made in predicting the distribution of herbaceous plants for introduction and cultivation, several key aspects still require improvement. First, methodologically, many studies continue to rely heavily on default model parameters (Liu et al., 2025; Xing et al., 2023; Zhao et al., 2025a), lacking systematic optimization tailored to the ecological traits of specific species. This oversimplification may lead to predictions that deviate from reality, thereby reducing their practical value for guiding introduction efforts. Second, regarding environmental variable selection, existing distribution models for herbaceous forage species often overemphasize climate factors (Liu et al., 2025; Xing et al., 2023; Xu et al., 2023b; Zhao et al., 2025a) while neglecting microenvironmental elements, including topography, soil conditions, vegetation indices, and human activity intensity, that directly influence cultivation success and establishment rates (Elith and Leathwick, 2009; Franklin, 2023). This narrow climatic focus inadequately captures the multidimensional niche requirements essential for translating distribution predictions into practical introduction strategies. Such a narrow focus fails to fully capture the actual habitat requirements of species, limiting the practical applicability of the predictions. Furthermore, most current studies concentrate on the conservation of natural species distributions (Wu et al., 2018; Zhang et al., 2023), with insufficient analysis of the spatiotemporal dynamics of suitable introduction areas under future climate scenarios. There is also a lack of systematic consideration for medium-to long-term introduction planning, which hinders the ability to meet the needs of modern, large-scale agricultural cultivation. These methodological and application limitations significantly restrict the effective translation and broader adoption of distribution prediction research in agricultural practice.

This study focuses on *Setaria palmifolia* (J. Konig) Stapf, a perennial C4 grass species belonging to the genus *Setaria* in the Poaceae family. As a C4 plant, it possesses a highly efficient photosynthetic pathway that confers superior water-use efficiency and high productivity potential compared to many C3 species, making it particularly advantageous in water-limited environments. Additionally, *S. palmifolia* shows distinctive ecological traits including strong shade tolerance and adaptation to warm and humid conditions, enabling its cultivation across diverse agroecological settings such as forest understory systems and subtropical marginal lands (Liao and Kao, 2023). These combined characteristics, namely high biomass production, water-use efficiency, shade tolerance, and climatic adaptability, position it as a uniquely promising forage resource for sustainable agricultural development in southern China. In this region, heterogeneous landscapes and climate change pressures require resilient and multi-purpose plant species.

The aim of this research is to systematically refine the methodology of species distribution modeling to scientifically assess its suitable cultivation areas in China and its responses to future climate change. Our specific objectives are threefold. First, we will construct a high-quality species distribution database by integrating multi-source data and applying rigorous quality control, thereby establishing a multidimensional evaluation index system that includes climate, topography, and human activities. Second, we will enhance the predictive performance of the MaxEnt model through parameter optimization to ensure the ecological plausibility and spatial accuracy of its outputs. Third, using the optimized model, we will predict suitable introduction areas under both current and future climate scenarios and systematically analyze their spatiotemporal dynamics. Based on these objectives, we propose three research hypotheses. First, the dominant environmental factors influencing the distribution of *S. palmifolia* are key constraints for its introduction site selection, and different combinations of these factors will determine the spatial pattern of suitable areas. Second, future climate change will significantly alter the spatial distribution of suitable cultivation areas for this species, manifesting as systematic changes in the extent, centroid location, and spatial connectivity of these areas. Third, the expansion pathways of suitable introduction zones will vary markedly under different emission scenarios, and these differences will directly influence the formulation of long-term cultivation plans and the selection of risk management strategies.

To address our research objectives, we employed a systematic methodology. We first obtained species occurrence records from authoritative databases, followed by rigorous deduplication and quality control. We then selected initial environmental variables from multiple dimensions (climate, topography, human activity) and performed collinearity diagnostics to filter the key variable set for modeling. The MaxEnt model was systematically calibrated by optimizing feature classes and regularization multipliers, with the optimal combination determined via grid search. Subsequently, the tuned model predicted suitable introduction areas for multiple timeframes and climate scenarios. These projections were integrated with centroid shift analysis, suitability classification, and spatial pattern change detection to comprehensively reveal spatiotemporal dynamics. This study establishes a practical framework from prediction to introduction, supporting sustainable plant resource utilization and quality agricultural development in China through precise suitable area identification, production layout optimization, and ecological restoration guidance.

2. Materials and methods

2.1. Acquisition and processing of species distribution data

This study constructed a species distribution dataset for *S. palmifolia* by systematically integrating multi-source data. Records were sourced from the Chinese Virtual Herbarium (CVH, http://www.cvh.org.cn/, accessed 9 August 2025), the Global Biodiversity Information Facility (GBIF, https://doi.org/10.15468/dl.8qxrfu, accessed 18 August 2025), the China National Knowledge Infrastructure (CNKI, https://www.cnki.net/, accessed 22 August 2025), and Google Scholar (https://ac.scmor.com/, accessed 25 August 2025). Initially, a total of 2778 non-duplicate distribution records were obtained (2642 from GBIF, 134 from CVH, and one each from CNKI and Google Scholar) were obtained. To reduce the impact of spatial autocorrelation on model prediction accuracy, we implemented a multi-step optimization process for the occurrence data. First, using ArcGIS 10.8, we created a 2.5′ grid covering the study area to serve as the basic unit for spatial filtering. Second, following the nearest-to-center principle, we retained only one representative point per grid cell. This approach effectively reduced sampling clustering bias while preserving the completeness of the distribution range. Third, we standardized the data format, saving the resulting 927 occurrence points (804 obtained from GBIF, 121 from CVH, and 1 each from CNKI and Google Scholar) (Fig. 1) as a.csv file to meet the input requirements of MaxEnt version 3.4.4 (available from http://biodiversityinformatics.amnh.org/open_source/maxent/, accessed 25 August 2025). This comprehensive processing workflow ensured spatial independence of the data and established a reliable foundation for the subsequent accurate construction of the species distribution model. Additionally, this study employed the base map of China from the Standard Map Service System of the Ministry of Natural Resources of China (Approval No. GS (2023)2762, accessed on 22 December 2023 at http://bzdt.ch.mnr.gov.cn/).

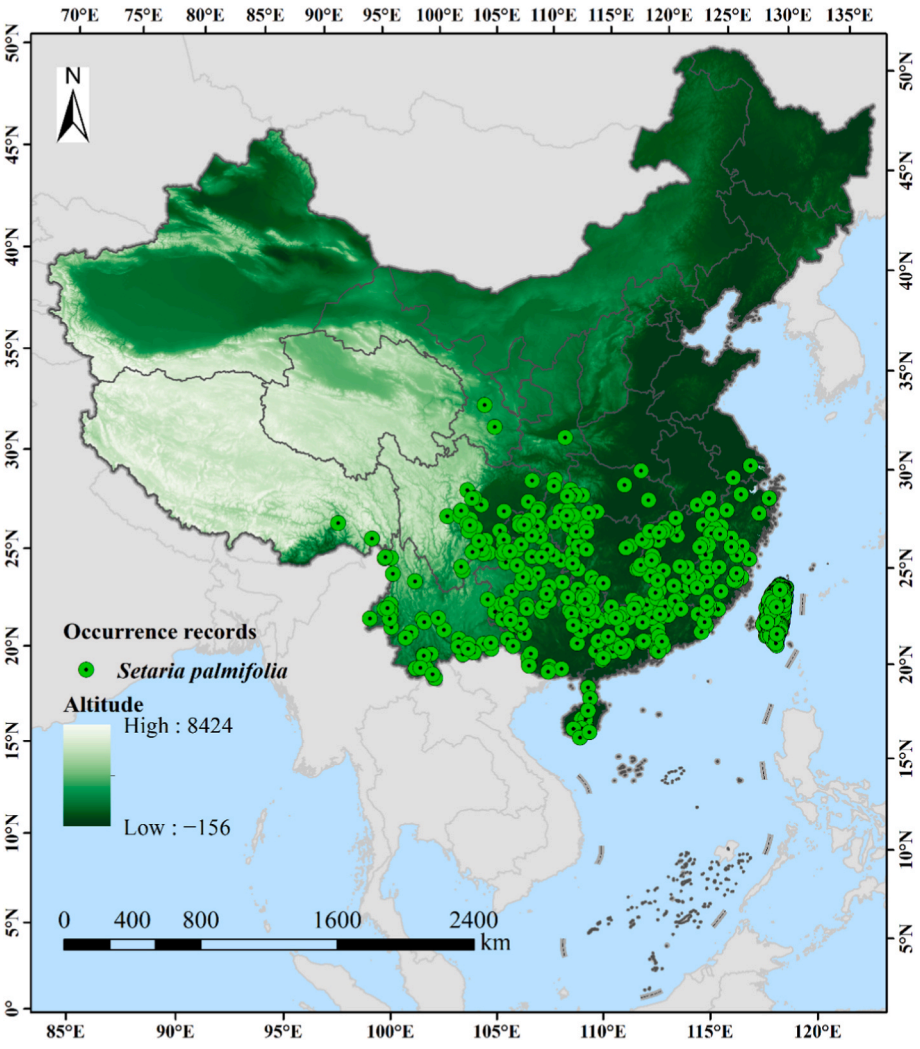

Fig. 1. Geographical distribution of the 927 occurrence records of *S. palmifolia* in China.

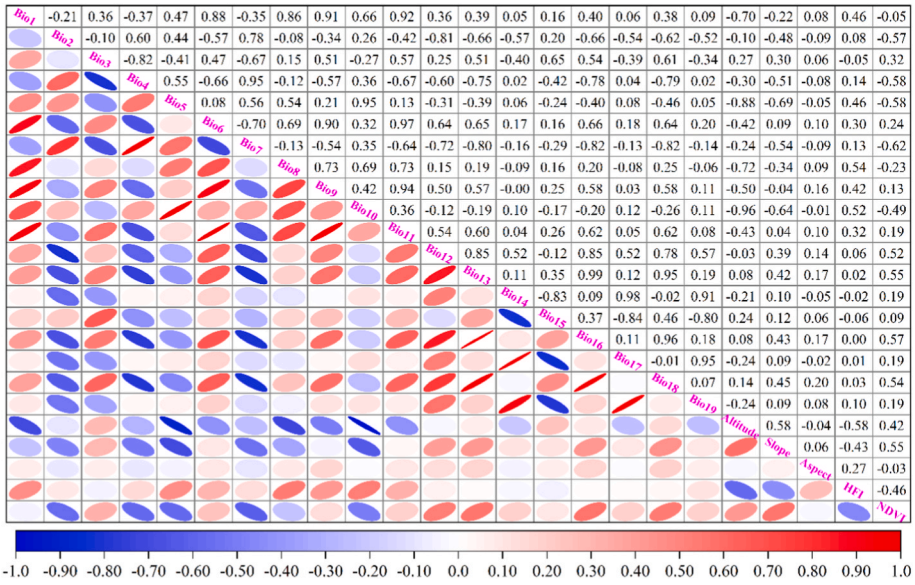

Fig. 2. Correlation matrix of the 24 environmental variables. Red indicates a positive correlation and blue indicates a negative correlation. Color saturation represents the absolute value of the correlation coefficient: darker colors indicate stronger correlations; lighter colors (approaching white) indicate correlations near zero.

2.2. Collection and screening of environmental variables

In selecting environmental variables, multiple drivers including climate, topography, vegetation, and human activity were comprehensively considered. A total of 24 initial variables were selected for building the species distribution model of *S. palmifolia* (Table S1). Specifically, 19 bioclimatic variables and elevation data were obtained from the WorldClim 2.1 platform (https://www.worldclim.org/, accessed 16 August 2025). Based on this elevation data, we derived two topographic factors, slope and aspect, using ArcGIS 10.8. Vegetation cover was characterized by the Normalized Difference Vegetation Index (NDVI) from the MODIS/Terra MOD13A3 product (Didan, 2015), while human activity intensity was represented by the Human Footprint Index (Mu et al., 2022). To assess future climate change impacts, we selected the BCC-CSM2-MR model from the Coupled Model Intercomparison Project Phase 6 (CMIP6), which is recognized as particularly suitable for studying climate change in China (Jin et al., 2024; Xin et al., 2020). We combined it with three Shared Socioeconomic Pathways (SSP), SSP126, SSP370, and SSP585, to predict distribution changes for the 2050s, 2070s, and 2090s.

To mitigate multicollinearity effects on model accuracy and interpretability, we performed Variance Inflation Factor (VIF) diagnosis and Spearman correlation analysis on all variables (Fig. 2) using R 4.2.2 with the usdm package (version 2.1-7) (Naimi, 2015). Following established best practices for ecological niche modeling (Dormann et al., 2013), screening criteria were set at VIF <10 and $|r| < 0.7$ to ensure retention of statistically independent variables. When two correlated variables exceeded these thresholds, we retained the variable with greater ecological relevance to *S. palmifolia*'s known habitat requirements (e.g., retaining Bio18 over Bio16 due to its direct relationship with growing season moisture availability). Ultimately, 10 environmental variables were included in the final model, covering four categories: climate (six variables), topography (two variables), human activity (one variable), and vegetation (one variable) (Table 1).

2.3. Optimization of model parameters

To enhance the accuracy and robustness of MaxEnt model predictions for the potential distribution of *S. palmifolia*, this study systematically optimized two key parameters: the feature classes (FC) and regularization multiplier (RM). These parameters jointly control model complexity and generalization ability(Yan et al., 2021), and optimizing them enhances the model's fit to the species-environment relationship, thereby yielding more ecologically plausible and spatially accurate predictions. Specifically, using R 4.2.2 and the ENMeval 2.0.4 package (Kass et al., 2021), we implemented a grid search strategy to evaluate model performance across different parameter combinations. We set the regularization multiplier from 0.5 to 4.0 in increments of 0.5. These multipliers were tested in combination with nine feature class schemes (L, H, LQ, LQH, LQHP, LQHPT, QHP, QHPT, HPT), which incorporate five feature function types: linear (L), quadratic (Q), product (P), threshold (T), and hinge (H) (Phillips and Dudík, 2008). The optimal parameter set was selected based on the corrected Akaike Information Criterion (AICc), following the principle of minimizing the AICc value (Muscarella et al., 2014). We applied the recommended threshold of Delta AICc ≤ 2, as proposed by Anderson and Gonzalez (2011).

Table 1
Environmental variables employed for modeling the potential distribution of *S. palmifolia*.

Category	Abbreviation	Environmental variables	Units	VIF
Bioclimatic	Bio2	Mean diurnal range (Mean of monthly)	°C	8.50
	Bio3	Isothermality (Bio2/Bio7) (× 100)		5.34
	Bio5	Max temperature of warmest month	°C	6.87
	Bio8	Mean temperature of wettest quarter	°C	4.85
	Bio18	Precipitation of warmest quarter	mm	3.99
	Bio19	Precipitation of coldest quarter	mm	2.31
Topographic	Aspect	Aspect	°	2.27
	Slope	Slope	°	1.17
Human	HFI	Human footprint index		2.15
Vegetation	NDVI	Normalized difference vegetation index		2.49

2.4. Model calibration and performance assessment

To simulate the potential suitable habitat of *S. palmifolia* under climate change, this study established an optimized MaxEnt modeling workflow based on 927 occurrence records. The specific procedure included several key steps. First, using stratified random sampling, we partitioned the data into training (75%) and validation (25%) sets. This approach ensured both environmental representativeness and statistical independence. Next, we implemented systematic parameter settings to enhance model performance: we applied cross-validation to improve internal robustness; used 10,000 background points to adequately characterize environmental backgrounds; set the regularization multiplier to 1.5 to balance model complexity; and selected the LQHPT feature combination to capture complex nonlinear ecological responses. After 10 replicate model runs, we integrated the results and generated a final logistic suitability probability raster, providing a standardized data foundation for subsequent multi-scenario analysis and spatial mapping.

To comprehensively evaluate the predictive capability of the optimized MaxEnt model, we employed three complementary metrics: the area under the curve (AUC) of the receiver operating characteristic (ROC) curve, true skill statistics (TSS), and Cohen's kappa coefficient (Kappa). AUC measures the model's ability to distinguish between species presence and background environments, with its accuracy categorized as follows: 0.5–0.6 (fail), 0.6–0.7 (poor), 0.7–0.8 (fair), 0.8–0.9 (good), and 0.9–1.0 (excellent) (Phillips and Dudík, 2008). TSS combines sensitivity and specificity to correct for random bias, and its evaluation criteria are: <0.4 (poor performance), 0.4–0.8 (good), and >0.8 (excellent) (Allouche et al., 2006). Kappa quantifies the agreement between predicted and actual distributions, where values < 0.4 indicate poor agreement, 0.4–0.75 represent good agreement, and >0.75 reflect excellent agreement (Xu et al., 2023a).

Model performance was evaluated using the Area Under the Curve (AUC) of the Receiver Operating Characteristic (ROC) curve. To elucidate the relationship between the occurrence probability of *S. palmifolia* and the three key environmental factors, we plotted single-factor response curves based on the final model outputs.

2.5. Categorization of habitat suitability

To accurately delineate the potential distribution range of *S. palmifolia*, this study adopted the 'Maximum Training Sensitivity Plus Specificity Logistic Threshold' (MTSPS) as the primary criterion for classifying suitable habitats. This threshold effectively balances model omission and commission errors while remaining insensitive to variations in species occurrence frequency, making it a widely recognized, robust approach in ecological niche modeling (Mechergui et al., 2025; Zhang et al., 2025). Based on the average suitability index (P) derived from 10 replicate model runs, we performed spatial classification in ArcGIS 10.8 using the Reclassify tool. Using the MTSPS threshold (0.1625) as the starting critical point, we subdivided habitat suitability into four ordered categories: non-suitable ($P < 0.1625$), low-suitable ($0.1625 \leq P < 0.3$), medium-suitable ($0.3 \leq P < 0.5$), and high-suitable ($P \geq 0.5$). This classification scheme preserves the statistical rigor of the MTSPS method while enhancing the ecological interpretability and visual communication of spatial suitability patterns.

2.6. Changes in the spatial pattern

Based on comparisons of suitable habitats under current and future climate scenarios, changes in species distribution ranges can be categorized into three types: retention areas (suitable in both current and future periods), loss areas (currently suitable but becoming unsuitable in the future), and expansion areas (currently unsuitable but becoming suitable in the future) (Liao et al., 2025; Zhao et al., 2025a). To quantitatively analyze the evolution of suitable habitats for *S. palmifolia* under future climate scenarios, this study conducted a multi-period spatial dynamic assessment in ArcGIS 10.8, using the average suitability probability (P) derived from 10 replicate MaxEnt model runs. First, using the MTSPS threshold (0.1625) as the cutoff point, we converted continuous suitability probability data, for both the current period and future scenarios (SSP126, SSP370, SSP585 across the 2050s, 2070s, and 2090s), into binary distribution layers. In these layers, a pixel value of 1 indicates a suitable area, while 0 indicates a non-suitable area. Next, we transformed the binary data for each period into polygon layers using the raster-to-vector tool. We then applied the "Intersect" overlay analysis tool to identify the spatial intersection between the suitable area vectors of each future period and the current distribution. Through this process, we constructed a spatial change map reflecting three dynamic categories: retention areas (1 → 1), loss areas (1 → 0), and expansion areas (0 → 1) (Xiang et al., 2025), thereby systematically revealing the spatiotemporal migration trajectory of the species' distribution range.

2.7. Centroid shift in suitable habitats

To quantitatively reveal the response characteristics of *S. palmifolia*'s suitable habitats to climate change, this study systematically analyzed the migration trajectory of its distribution centroid based on the average suitability probability (P) derived from 10 replicate MaxEnt model runs. The specific procedure included several steps. First, within the ArcGIS 10.8 platform, we applied a threshold of 0.1625 to convert the probability raster into a binary map. This process delineated the boundaries between suitable and non-suitable habitats, and the resulting raster was then converted into vector polygon data. Next, using the spatial statistics tool, we calculated the geometric center point to accurately extract the centroid coordinates of the suitable habitat polygons for each period and climate scenario. Finally, using the changes in the latitude and longitude of these centroid positions across different time periods, we applied the Euclidean distance algorithm to quantify both the distance and direction of migration. This approach systematically characterized the spatial displacement trend driven by climate change.

3. Results

3.1. Model optimization and accuracy evaluation

To optimize the MaxEnt model for *S. palmifolia*, this study employed Delta AICc as the core evaluation metric. An initial assessment revealed that the default parameter set (RM = 1, FC = LQHP) yielded a Delta AICc value of 56.35 (Fig. 3), significantly exceeding the recommended threshold (ΔAICc ≤2). This indicated a substantial risk of overfitting. To address this, based on 927 occurrence records and 10 environmental variables, we conducted a systematic grid search of the parameter space (RM: 0.5–4, increment 0.5; FC: L, Q, H, P, T, and their combinations) using the ENMeval package (v2.0.4). The parameter optimization process identified an optimal combination (RM = 1.5, FC = LQHPT) with a ΔAICc value of 0, demonstrating that this model provides the best fit among tested configurations while effectively avoiding overfitting. Model performance validation showed consistent AUC values of 0.935 both before and after optimization (Fig. S1a and b), meeting the "excellent" standard (AUC ≥0.9). This confirms that the optimized model maintains very high predictive accuracy while achieving a substantial improvement in robustness. According to conventional evaluation standards, the optimized model performed excellently in terms of its True Skill Statistic (TSS = 0.817) and well in terms of its Kappa coefficient (0.515).

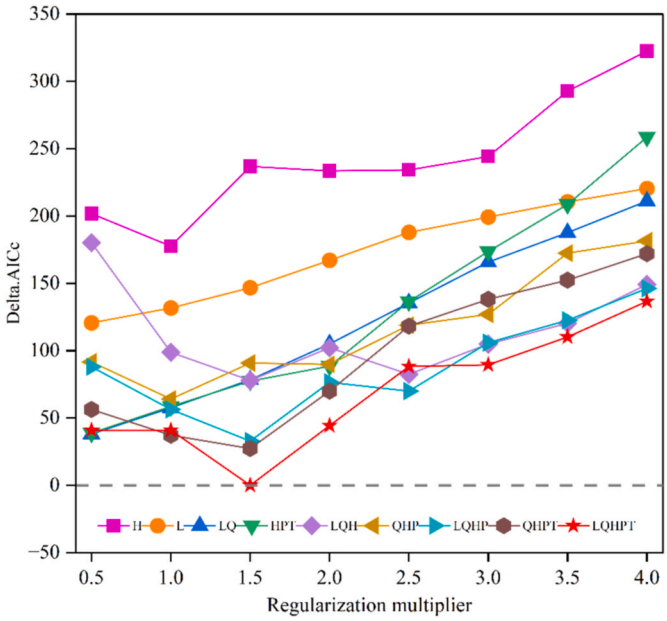

Fig. 3. Distribution of delta AICc values across FCs for *S. palmifolia*. The dashed line indicates the zero-reference level. FCs are represented as follows: L (Linear), Q (Quadratic), H (Hinge), P (Product), T (Threshold).

3.2. Dominant environmental factors

This study utilized the optimized MaxEnt model to systematically analyze the influence of ten environmental factors on the potential geographic distribution of *S. palmifolia*, integrating both variable contribution rates and jackknife test results. As shown in Fig. 4a, the environmental variables are listed in descending order of contribution: precipitation of the warmest quarter (Bio18, 37.1%), precipitation of the coldest quarter (Bio19, 36.6%), mean diurnal range (Bio2, 19.7%), human footprint index (HFI, 1.8%), slope (1.3%), normalized difference vegetation index (NDVI, 1.3%), max temperature of the warmest month (Bio5, 0.8%), isothermality (Bio3, 0.7%), mean temperature of the wettest quarter (Bio8, 0.4%), and aspect (0.3%). In terms of factor categories, climatic factors collectively accounted for 95.3% of the total contribution, followed by human activity factors (1.8%), topographic factors (1.6%), and vegetation factors (NDVI, 1.3%). The jackknife test of regularized training gain (Fig. 4b) further indicated that, when used in isolation, the top five variables with the highest gain values were Bio18, Bio2, Bio19, NDVI, and HFI. According to the conventional screening criterion of cumulative contribution exceeding 85%, Bio18, Bio19, and Bio2 together explained 93.4% of the variation in the species' suitable distribution. This highlights their decisive role in shaping the potential geographic distribution of *S. palmifolia* in China, identifying water availability during both growing (Bio18: warmest quarter) and dormant (Bio19: coldest quarter) seasons, coupled with thermal stability (Bio2), as the core climatic drivers. This finding aligns with the species' physiological requirements as a C4 perennial grass requiring consistent moisture throughout the year for sustained productivity.

The analysis revealed that the effect of Bio18 on occurrence probability initially increased and then gradually decreased. Specifically, as precipitation increased from 0 mm to 545.13 mm, the probability rose rapidly from 0.21 to 0.55. It continued to climb gradually to a peak of 0.66 within 545.14 – 1775.10 mm, then slowly declined to 0.61 in the 1775.11 – 2390.08 mm range and stabilized after exceeding 2390.08

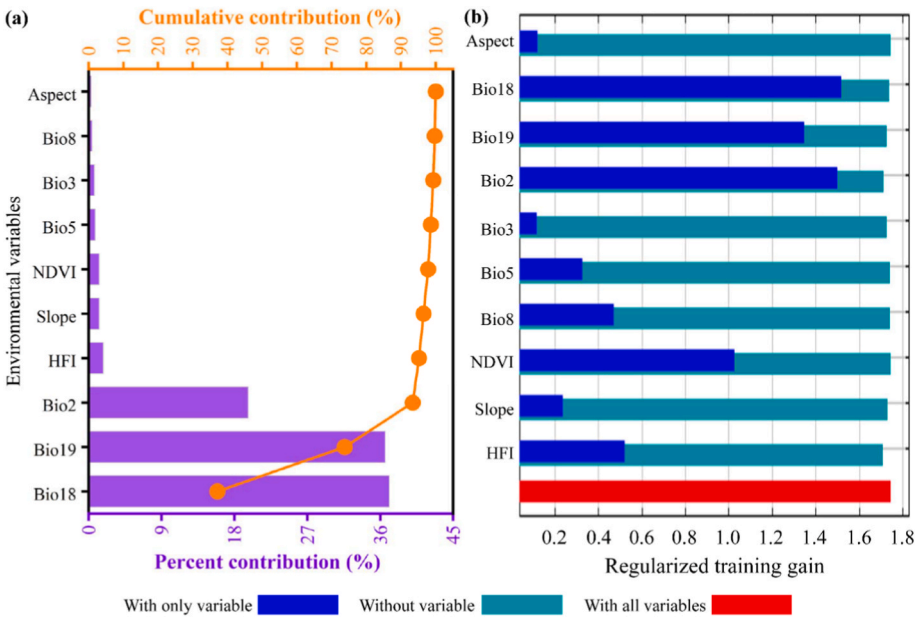

Fig. 4. Relative importance of environmental predictors for *S. palmifolia* in the MaxEnt model: (a) percent contribution and (b) jackknife test of regularized training gain.

mm (Fig. 5a). In contrast, Bio19 exhibited a consistently positive response: probability increased rapidly from 0.11 to 0.52 as precipitation rose from 0 mm to 68.61 mm; it further increased to 0.59 in the 68.62 – 192.41 mm range; and then slowly reached its maximum probability of 0.62 within 192.42 – 909.98 mm (Fig. 5b). Meanwhile, Bio2 showed a clear negative effect: probability remained stable at 0.74 within the 3.65 – 4.88 °C range; it then dropped sharply to 0.09 as the temperature increased from 4.89 °C to 13.52 °C; subsequently, it declined slowly to 0.02 in the 13.53 – 18.86 °C range and remained nearly constant beyond 18.86 °C (Fig. 5c).

3.3. Potential distribution of S. palmifolia under contemporary climate conditions

Under current climatic conditions, the total potentially suitable habitat for *S. palmifolia* in China covers approximately 177.22 × 10^4 km^2, accounting for about 18.46% of the country's total land area (Fig. 6). The highly suitable areas, spanning about 12.20 × 10^4 km^2 (1.27%), are concentrated primarily in Taiwan Province and Hainan Province, as well as in southern Yunnan Province, central Guangxi Zhuang Autonomous Region, western Guangdong Province, and western Chongqing Municipality. Moderately suitable areas cover approximately 86.82 × 10^4 km^2 (9.04%) and are widely distributed across multiple regions, including Fujian Province, Jiangxi Province, southern Zhejiang Province, southern Anhui Province, central and southern Hunan Province, western Hubei Province, central Guizhou Province, eastern Sichuan Province, eastern and western Guangxi Zhuang Autonomous Region, and southeastern Xizang Autonomous Region. In contrast, low-suitable areas extend over about 78.20 × 10^4 km^2 (8.15%) and are fragmented and distributed across central Yunnan Province, eastern and western Guizhou Province, central Hunan Province, eastern and western Hubei Province, eastern Sichuan Province, central and southern Anhui Province, northern Zhejiang Province, and southern Henan Province.

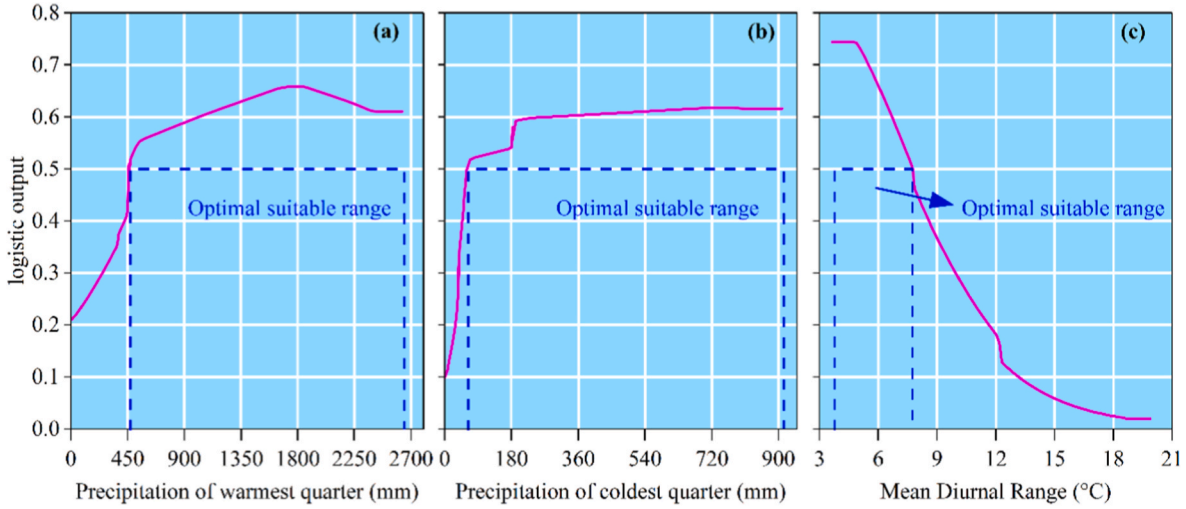

Fig. 5. Mean response curves of *S. palmifolia* to critical environmental variables, depicting the probability of presence (blue line, mean of 10 replicates) and the optimal suitability range (purple dashed lines). (a) Precipitation of Warmest Quarter (Bio18); (b) Precipitation of Coldest Quarter (Bio19); (c) Mean Diurnal Range (Bio2).

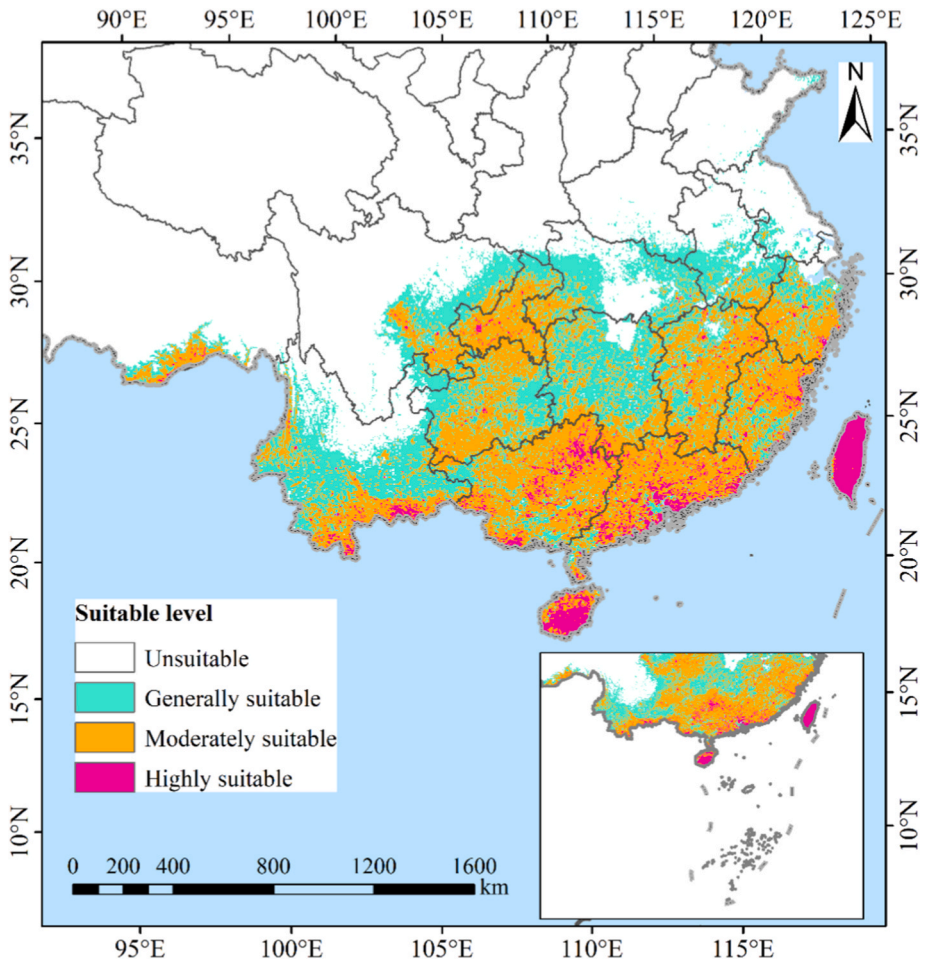

Fig. 6. Potential distribution of *S. palmifolia* in China under the baseline climate scenario.

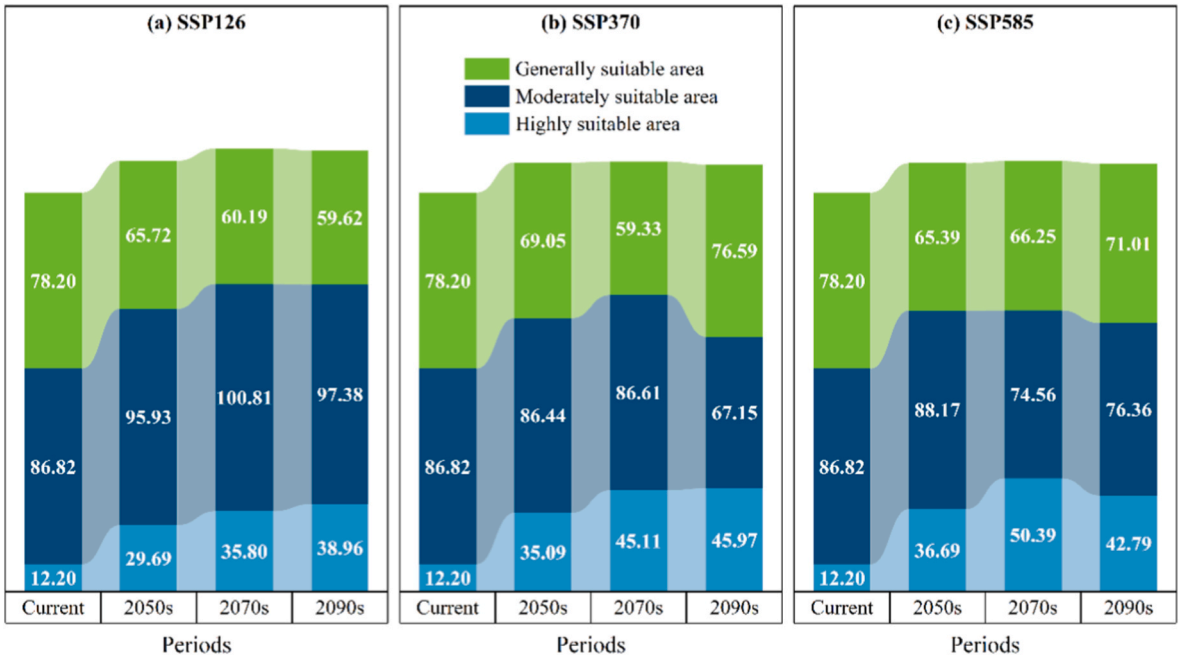

Fig. 7. Projected shift in the distribution of suitable habitat for *S. palmifolia* from the present to the 2090s under climate change scenarios (unit: 10^4 km^2).

3.4. Future potential distribution of S. palmifolia in China under climate change scenarios

Under the SSP126 future climate scenario, the potential suitable habitat of *S. palmifolia* in China is projected to expand continuously. By the 2050s, the total suitable area is expected to reach 191.34 × 10^4 km^2, accounting for approximately 19.93% of the country's land area. This total comprises low-, medium-, and high-suitability areas covering 65.72 × 10^4 km^2, 95.93 × 10^4 km^2, and 29.69 × 10^4 km^2, respectively (Fig. 7). At this stage, high-suitability zones are mainly distributed across Taiwan Province, Hainan Province, Jiangxi Province, southern Yunnan Province, northeastern Guangxi Zhuang Autonomous Region, northern Guangdong Province, eastern Fujian Province, central Hunan Province, southeastern Hubei Province, western Zhejiang Province, and western Chongqing Municipality (Fig. 8a). By the 2070s, the total suitable area further increases to 196.80 × 10^4 km^2 (20.50% of China's land area), with low-, medium-, and high-suitability areas covering 60.19 × 10^4 km^2, 100.81 × 10^4 km^2, and 35.80 × 10^4 km^2, respectively (Fig. 7). The extent of high-suitability areas remains largely stable, still concentrated in Taiwan Province, Hainan Province, Jiangxi Province, and Zhejiang Province, as well as parts of southern Yunnan Province, northeastern Guangxi Zhuang Autonomous Region, northwestern Guangdong Province, eastern Fujian Province, central Hunan Province, southeastern Hubei Province, and western Chongqing Municipality (Fig. 8d). By the 2090s, the total suitable area slightly decreases to 195.96 × 10^4 km^2 (20.41%), yet high-suitability areas continue to expand, reaching 38.96 × 10^4 km^2, while medium- and low-suitability areas cover 97.38 × 10^4 km^2 and 59.62 × 10^4 km^2, respectively (Fig. 7). In addition, high-suitability zones show a tendency to extend into western and southeastern Zhejiang Province, western Jiangxi Province, and northern Chongqing Municipality (Fig. 8g).

Under the SSP370 scenario, the total suitable habitat area remains generally stable, though its internal structure undergoes notable changes. By the 2050s, the total area reaches 190.58 × 10^4 km^2 (19.85% of China's land area), comprising low-, medium-, and high-suitability areas of 69.05 × 10^4 km^2, 86.44 × 10^4 km^2, and 35.09 × 10^4 km^2, respectively (Fig. 7). High-suitability areas during this period are mainly located in Taiwan Province, Hainan Province, Jiangxi Province, Zhejiang Province, southern Yunnan Province, northeastern Guangxi Zhuang Autonomous Region, northern Guangdong Province, eastern Fujian Province, southeastern Hubei Province, and central Hunan Province (Fig. 8b). By the 2070s, the total area increases slightly to 191.05 × 10^4 km^2 (19.90%), while high-suitability zones expand markedly to 45.11 × 10^4 km^2, extending further westward into western Chongqing Municipality (Fig. 8e). In the 2090s, the total area declines modestly to 189.71 × 10^4 km^2 (19.76%), yet high-suitability areas continue to grow, reaching 45.97 × 10^4 km^2. Their distribution also shows a northward and eastward shift, with new expansions into southern Anhui Province and more concentrated coverage along the Hunan–Hubei border (Fig. 8h).

Under the SSP585 scenario, the total suitable area remains relatively stable, but its internal structure continues to adjust. By the 2050s, the

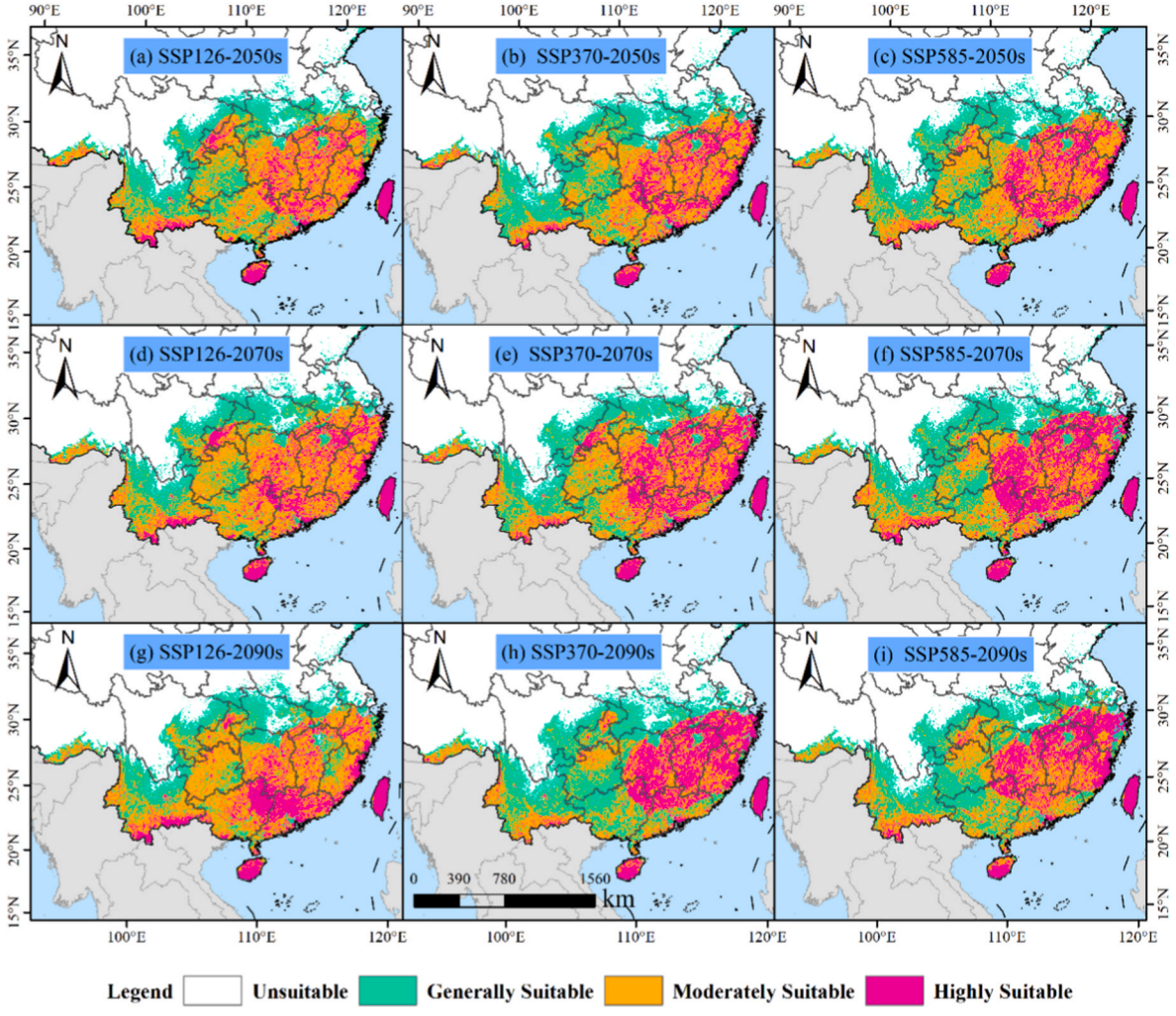

Fig. 8. Integrated projection of suitable habitat for *S. palmifolia* in China under future climate scenarios.

total area is 190.25 × 10^4 km^2 (19.82% of China's land area), with low-, medium-, and high-suitability areas covering 65.39 × 10^4 km^2, 88.17 × 10^4 km^2, and 36.69 × 10^4 km^2, respectively (Fig. 7). High-suitability zones are mainly found in Taiwan Province, Hainan Province, northern Jiangxi Province, southern Yunnan Province, northern Guangxi Zhuang Autonomous Region, northern Guangdong Province, northern and eastern Fujian Province, western Zhejiang Province, southern Anhui Province, central Hunan Province, southeastern Hubei Province, and central Chongqing Municipality (Fig. 8c). By the 2070s, the total area increases slightly to 191.20 × 10^4 km^2 (19.92%), while high-suitability areas expand significantly to 50.39 × 10^4 km^2, stretching northward into northern Zhejiang Province and forming more continuous clusters in southeastern Hubei Province and central Hunan Province (Fig. 8f). By the 2090s, the total area declines slightly to 190.15 × 10^4 km^2 (19.81%), and high-suitability areas decrease to 42.79 × 10^4 km^2. Although this represents a decrease compared to the 2070s, it remains notably higher than the 2050s level. Spatially, the distribution remains relatively stable, continuing to cover major suitable regions in eastern, central, and southwestern China (Fig. 8i).

3.5. Spatial-temporal dynamics of suitable habitats under climate change scenarios

Under the SSP126 future climate scenario, the suitable habitat of *S. palmifolia* remains generally stable despite minor fluctuations across periods, showing a consistent long-term expansion trend (Fig. 9). Specifically, by the 2050s (Fig. 9a; Table 2), the retained area is 174.98 × 10^4 km^2 (retention rate: 90.54%), with a loss area of only 2.09 × 10^4 km^2 (loss rate: 1.08%) and an expansion area of 16.18 × 10^4 km^2 (expansion rate: 8.37%). By the 2070s (Fig. 9d; Table 2), the retained area increases slightly to 176.51 × 10^4 km^2 (89.42%), while the loss area further decreases to 0.59 × 10^4 km^2 (0.30%), and the expansion area continues to grow to 20.30 × 10^4 km^2 (10.28%). In the 2090s (Fig. 9g; Table 2), the retained area is 175.95 × 10^4 km^2 (89.33%), with a slight rebound in loss area to 1.12 × 10^4 km^2 (0.57%), while the expansion area remains at 19.91 × 10^4 km^2 (10.11%).

Under the SSP370 scenario, the species' suitable habitat exhibits a trend of gradually decreasing retention area, progressively increasing loss area, and moderately fluctuating expansion area (Fig. 9). In the 2050s (Fig. 9b; Table 2), the retained area is 175.63 × 10^4 km^2 (91.49%), with a loss area of 1.47 × 10^4 km^2 (0.77%) and an expansion area of 14.87 × 10^4 km^2 (7.75%). By the 2070s (Fig. 9e; Table 2), the retained area declines to 174.38 × 10^4 km^2 (90.14%), the loss area rises to 2.72 × 10^4 km^2 (1.40%), and the expansion area increases to 16.35 × 10^4 km^2 (8.45%). By the 2090s (Fig. 9h; Table 2), the retained area further decreases to 173.59 × 10^4 km^2 (89.95%), the loss area continues to grow to 3.50 × 10^4 km^2 (1.81%), and the expansion area slightly declines to 15.90 × 10^4 km^2 (8.24%).

Under the SSP585 scenario, the overall pattern remains relatively stable, with the three-area metrics showing minor fluctuations but no clear unidirectional trend (Fig. 9). In the 2050s (Fig. 9c; Table 2), the retained area is 174.18 × 10^4 km^2 (90.25%), with a loss area of 2.92 ×

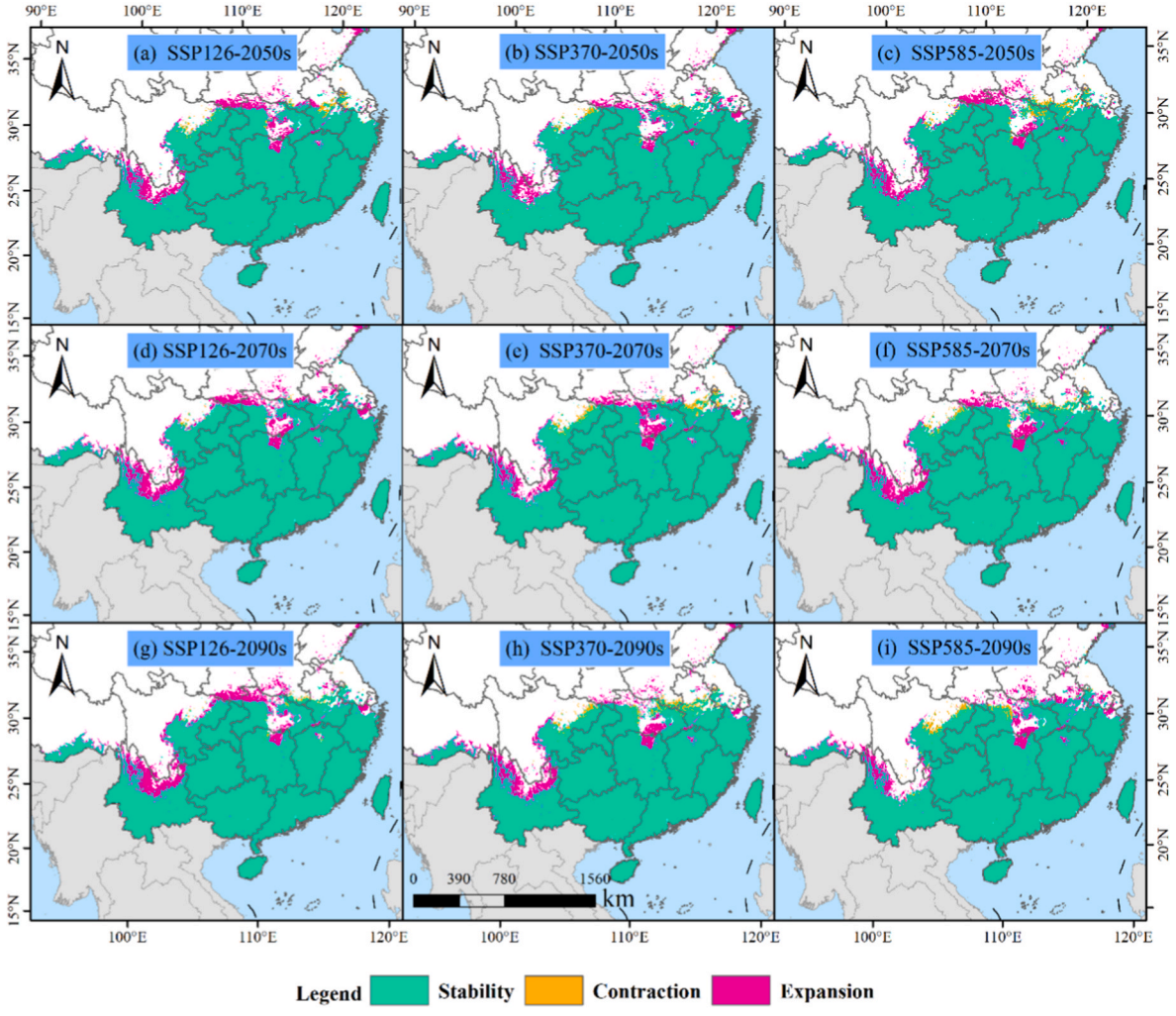

Fig. 9. Changes in stable, lost, and gained areas of *S. palmifolia* distribution under different climate change scenarios.

Table 2
Area changes in suitable habitat for *S. palmifolia* in response to various projection scenarios.

Scenario-period	Area (10^4 km^2)			Rate of change (%)		
	Stability	Contraction	Expansion	Stability	Contraction	Expansion
SSP126-2050s	174.98	2.09	16.18	90.54	1.08	8.37
SSP126-2070s	176.51	0.59	20.30	89.42	0.30	10.28
SSP126-2090s	175.95	1.12	19.91	89.33	0.57	10.11
SSP370-2050s	175.63	1.47	14.87	91.49	0.77	7.75
SSP370-2070s	174.38	2.72	16.35	90.14	1.40	8.45
SSP370-2090s	173.59	3.50	15.90	89.95	1.81	8.24
SSP585-2050s	174.18	2.92	15.90	90.25	1.51	8.24
SSP585-2070s	174.70	2.40	16.26	90.35	1.24	8.41
SSP585-2090s	174.58	2.50	15.42	90.69	1.30	8.01

10^4 km^2 (1.51%) and an expansion area of 15.90 × 10^4 km^2 (8.24%). By the 2070s (Fig. 9f; Table 2), the retained area increases slightly to 174.70 × 10^4 km^2 (90.35%), the loss area decreases to 2.40 × 10^4 km^2 (1.24%), and the expansion area rises modestly to 16.26 × 10^4 km^2 (8.41%). In the 2090s (Fig. 9i; Table 2), the retained area stabilizes at 174.58 × 10^4 km^2 (90.69%), the loss area increases slightly to 2.50 × 10^4 km^2 (1.30%), and the expansion area drops back to 15.42 × 10^4 km^2 (8.01%).

3.6. Centroid transfer of S. palmifolia under multiple climatic scenarios

The current distribution centroid of *S. palmifolia* in China is located in Wuyang Town, Suining County, Shaoyang City, Hunan Province (110°20′E, 26°45′N) (Fig. 10), and under different future climate scenarios, it exhibits clear migration patterns. Under the SSP126 scenario, the centroid first shifts northwest by approximately 34.28 km by the 2050s, reaching Jiangbao Village, Gaoyi Township, Huitong County, Huaihua City (110°05′E, 26°57′N). It then moves northeast by about 11.97 km by the 2070s, arriving at Longchuantang Yao Ethnic Township, Hongjiang City (110°08′E, 27°03′N). By the 2090s, it migrates southwest by approximately 10.07 km, finally stabilizing at Ruoshui Town, Huitong County (110°02′E, 27°01′N). In contrast, under the SSP370 scenario, the centroid moves northwest by about 27.08 km by the 2050s to Matang Miao and Yao Ethnic Township, Suining County (110°12′E, 26°57′N). It then continues shifting southwest, reaching Dashi Village, Gaoyi Township (110°05′E, 26°56′N) and later Tuanhe Town (109°59′E, 26°52′N), with a cumulative migration distance of approximately 25.14 km. Notably, under the SSP585 scenario, the centroid displays a more complex trajectory. It first migrates northwest by about 37.07 km by the 2050s to Baishi Village, Gaoyi Township, Huitong County (110°02′E, 26°56′N). It then shifts slightly southwest by approximately 4.98 km by the 2070s to Jinziyan Dong and Miao Ethnic

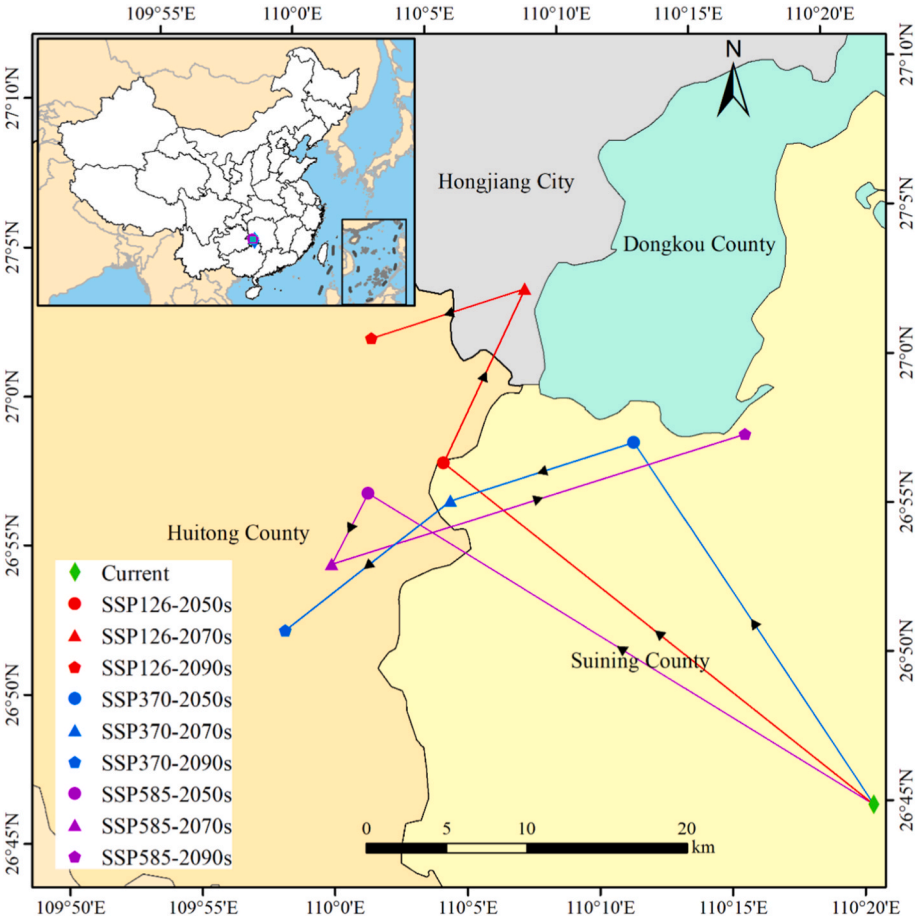

Fig. 10. Centroid trajectories across the suitable habitat of *S. palmifolia* under climate change.

Township (110°00′E, 26°54′N). However, by the 2090s, it reverses direction, moving northeast by about 27.10 km to Shuikou Township, Suining County (110°16′E, 26°58′N).

4. Discussion

4.1. Model calibration and performance assessment for S. palmifolia

The predictive capability and reliability of species distribution models are highly dependent on their parameter configuration (Hallgren et al., 2019). In this study, we conducted systematic parameter optimization of the MaxEnt model to address a common challenge in ecological niche modeling: the overreliance on default parameter settings, which may introduce excessive model complexity and overfitting risks (Kass et al., 2021). This methodological consideration aligns with the argument of Warren and Seifert (2011), who suggested that unadjusted default models may fail to achieve an optimal balance between predictive accuracy and generalization ability. Using an AICc-based grid search approach (Li et al., 2020), we identified the optimal parameter set (RM = 1.5, FC = LQHPT). This process adhered to the principle of parsimony in model selection, aiming to identify the simplest yet most effective explanation for species–environment relationships, rather than pursuing an extreme fit to the training data (Burnham and Anderson, 2004). This optimization strategy significantly improved model robustness, ensuring that the resulting suitability maps better reflect true ecological patterns and thereby providing a more reliable scientific basis for subsequent introduction planning.

In terms of model performance evaluation, this study employed a multi-metric validation framework comprising AUC, TSS, and Kappa (Allouche et al., 2006). Although the AUC and TSS values indicated exceptionally high discriminative ability (Phillips and Dudík, 2008), the Kappa coefficient of 0.515 suggested that there was still room for improvement in the agreement between predicted and actual distributions (Landis and Koch, 1977). This discrepancy may stem from unavoidable spatial sampling bias in species occurrence data, which can influence model evaluation outcomes (Veloz, 2009). To address this issue, future studies could adopt strategies such as spatial block cross-validation to more rigorously assess model performance in unsampled areas and its transferability (Roberts et al., 2017). Overall, this model calibration exercise not only confirms the importance of parameter optimization for enhancing the practical value of MaxEnt models, but also reflects the ongoing trend in species distribution modeling toward greater reproducibility, transparency, and interpretability (Muscarella et al., 2014).

4.2. Distributional stasis and internal suitability reorganization as a response mechanism

A central contribution of this study is the identification of a response pattern we term distributional stasis with internal suitability reorganization in *S. palmifolia*'s response to climate change. While the total suitable area remains remarkably stable across all future scenarios, ranging from 177.22×10^4 to 196.80×10^4 km^2, the internal structure undergoes profound transformation. Specifically, highly suitable habitat expands from 12.20×10^4 km^2 under current conditions to between 29.69×10^4 and 50.39×10^4 km^2 depending on emission scenarios, representing a 2.4-to-4.1-fold increase. This finding challenges the conventional poleward shift paradigm that has long dominated climate change biogeography (Parmesan and Yohe, 2003). Instead, our results align with the emerging concept of distributional stasis (Bowler et al., 2017; Zhu et al., 2012), which posits that many species respond to climate change not through large scale latitudinal or elevational shifts, but through local adjustments within their existing range and a restructuring of internal suitability patterns.

This mechanism of internal reorganization arises from heterogeneous changes in climatic factors and their complex, nonlinear interactions with species specific niche thresholds. At the same time, microclimatic heterogeneity generated by complex topography offers local refugia, allowing species to track suitable conditions through short distance migration. This process manifests as relative range stability at broader spatial scales (Dobrowski, 2011). Importantly, future combinations of climatic variables may extend beyond current climatic space, resulting in novel climates that could compel species into unconventional distributional responses, further accentuating internal suitability reorganization over simple boundary shifts (Williams and Jackson, 2007).

We propose the term suitability turnover to describe this phenomenon, a metric that captures the simultaneous expansion of high suitability areas and contraction of low suitability zones within a stable total range. To our knowledge, this study provides the first quantitative documentation of suitability turnover in a C4 forage grass species across multiple SSP scenarios and time slices. Emerging evidence from diverse taxa supports this interpretation. For example, Cui et al. (2025) demonstrated that *Caragana versicolor* shrub expansion on the Tibetan Plateau was initially enhanced by moderate warming but subsequently constrained by climate extremes, highlighting how realized distribution changes arise from complex interactions between mean climate shifts and extreme events. Similarly, Román-Palacios and Wiens (2020) showed that across diverse taxa, local persistence within existing ranges often better characterizes climate responses than wholesale range shifts. The internal suitability reorganization we observe may reflect such nonlinear responses to combined changes in seasonal precipitation and temperature variability. This finding shifts the focus from simple range boundary mapping to internal suitability dynamics, offering a more nuanced framework for climate adaptive species management.

4.3. Empirical evidence for hierarchical filtering of non-climatic factors

While many species distribution modeling studies either exclude non-climatic variables or treat them as minor contributors, this study quantitatively tested the hierarchical filtering hypothesis (Soberón and Nakamura, 2009) using an optimized MaxEnt framework that integrated climate, topography, vegetation, and human activity variables. Our results show that climatic factors, specifically Bio18, Bio19, and Bio2, collectively account for 93.4% of the model's explanatory power at the national scale. However, the jackknife tests reveal that the Human Footprint Index (HFI, 1.8%) and NDVI (1.3%) retain independent regularized training gain when used in isolation, indicating their non negligible role as secondary filters.

This finding has two important implications. First, it empirically validates the hierarchical filtering hypothesis for a forage grass species. Broad scale climate conditions act as the primary filter, determining the fundamental niche, while local non-climatic factors serve as secondary filters that modulate realized distribution at finer scales (Pearson and Dawson, 2003). This outcome aligns with the hierarchical filtering hypothesis in niche theory, which proposes that species distributions at broad spatial scales are primarily constrained by regional climate conditions. Local non-climatic factors act as secondary filters whose influence may be obscured by dominant climatic signals in macro scale analytical models (Soberón and Nakamura, 2009). Thus, our conclusions do not negate the ecological relevance of non-climatic factors but rather clarify the scale at which they operate.

Second, this finding provides practical guidance for introduction planning. While climate suitability maps identify potential regions, successful establishment in expansion areas will depend on local human disturbance levels and vegetation conditions, a critical insight often overlooked in climate only SDM studies (Di Marco et al., 2018; He et al., 2009). The independent explanatory power of HFI and NDVI in jackknife tests suggests their potential importance at finer, local scales in influencing species establishment and population persistence. This finding reflects a phenomenon increasingly documented through observational studies. For instance, Zhao et al. (2025b) suggested that

tropical bird range expansions detected through field observations were shaped by habitat modification and vegetation cover, factors often secondary in broad scale climate models. This suggests that while our modeling identifies climatically suitable zones for *S. palmifolia*, successful introduction and population persistence in expansion areas will depend on local human disturbance levels and vegetation conditions.

4.4. Non-linear and multi-directional centroid migration trajectories

Contrary to the common expectation of unidirectional poleward or upward centroid shifts (Lenoir et al., 2017; Parmesan and Yohe, 2003), our analysis reveals complex, non-linear migration trajectories that vary markedly across SSP scenarios. Under SSP126, the centroid first shifts northwest by 34.28 km by the 2050s, then northeast by 11.97 km by the 2070s, and finally southwest by 10.07 km by the 2090s. Under SSP370, the centroid moves northwest by 27.08 km by the 2050s and then continues shifting southwest with a cumulative migration distance of approximately 25.14 km. Under SSP585, the centroid migrates northwest by 37.07 km by the 2050s, followed by a slight southwest shift of 4.98 km by the 2070s, and then a pronounced northeast reversal of 27.10 km by the 2090s.

This non-linear behavior challenges the prevailing assumption that climate change drives simple directional range shifts. Instead, our results suggest that local microclimatic refugia and water temperature interactions, rather than unidirectional temperature increase alone, drive the species' future redistribution (Dobrowski, 2011; Keppel et al., 2012). The complexity of distribution centroid migration further illustrates these nonlinear dynamics. The non-unidirectional trajectories of *S. palmifolia*'s centroid challenge the conventional poleward shift hypothesis, underscoring the decisive influence of local scale environmental filters and the co-variation of multiple climatic factors (Lenoir et al., 2017). Rather than responding simply to mean temperature increases, centroid movement reflects spatiotemporal differentiation of combined effects from extreme events and water stress (Garcia et al., 2014), modulated by microclimate refugia in complex terrain (Keppel et al., 2012). This mechanistic understanding aligns with emerging evidence that species' range dynamics under climate change are shaped by interactions between broad scale climate shifts and local scale buffers (Cui et al., 2025).

The scenario dependent variability further indicates that different emission pathways produce qualitatively different spatial outcomes, which has direct implications for long term introduction planning. For instance, under SSP585 by the 2070s, the northeastward reversal suggests that novel climate combinations (Williams and Jackson, 2007) may create unexpected suitable conditions in previously marginal areas. To our knowledge, this study provides the first documentation of non-linear, multi-directional centroid migration for a forage grass species under contrasting SSP scenarios, highlighting the need for dynamic, scenario adaptive management strategies rather than static conservation plans.

4.5. Limitations of this study and future research directions

This study has three key limitations. First, the selection of environmental variables remains dominated by climatic factors, while localized non-climatic drivers such as soil properties and interspecific competition are not fully incorporated. This limitation reduces the model's predictive accuracy at micro-habitat scales. Second, although parameter optimization effectively mitigated overfitting, spatial sampling bias in the occurrence data of *S. palmifolia* persists. This leaves room for improvement in model predictive consistency, as reflected in metrics such as the Kappa coefficient. Third, the current modeling framework does not account for the species' actual dispersal capacity or landscape resistance, which may lead to overestimation of the ecological accessibility of future suitable habitats.

To address these gaps, future research should focus on developing multi-scale, multi-factor integrated habitat models that incorporate key variables such as soil attributes and biotic interactions. Future studies should also adopt validation strategies like spatial block cross-validation to enhance model generalizability and transferability to unsampled regions. Furthermore, integrating dispersal models and landscape connectivity analysis could provide a more realistic assessment of the actual expansion pathways and conservation feasibility of *S. palmifolia* under climate change.

5. Conclusion

This study systematically predicted the potential distribution patterns of *S. palmifolia* in China under both current and future climate scenarios. By optimizing the MaxEnt model, we determined that its distribution is primarily controlled by seasonal precipitation, specifically precipitation of the warmest and coldest quarters, and the mean diurnal temperature range. Our findings reveal that although the total suitable habitat area remains stable under future scenarios, it undergoes significant internal reorganization: the extent of highly suitable areas continues to expand, and the distribution centroid shifts along complex trajectories, challenging the traditional poleward shift paradigm. This highlights microclimatic heterogeneity and water-thermal interactions as pivotal mechanisms. Our work delivers critical insights for forecasting ecological responses to climate change and creates a science-based framework for the strategic cultivation and conservation of *S. palmifolia* as a forage resource, pinpointing key areas for protection and expansion. Integrating soil and dispersal data is a vital next step for refining these predictions. The spatially explicit framework developed here offers a replicable methodology for assessing climate-driven habitat reorganization in economically important plant species, supporting evidence-based policy formulation for agricultural sustainability in China and comparable regions globally.

CRediT authorship contribution statement

Yangzhou Xiang: Writing – review & editing, Writing – original draft, Visualization, Validation, Software, Methodology, Investigation, Funding acquisition, Formal analysis, Data curation, Conceptualization. **Suhang Li:** Writing – review & editing, Visualization, Validation, Formal analysis, Data curation, Conceptualization. **Ying Liu:** Writing – review & editing, Resources, Methodology, Conceptualization. **Qiong Yang:** Writing – review & editing, Data curation, Conceptualization. **Jinxin Zhang:** Writing – review & editing, Resources, Project administration, Investigation, Funding acquisition, Data curation, Conceptualization. **Bin Yao:** Writing – review & editing, Resources, Project administration, Investigation, Funding acquisition, Conceptualization. **Yuan Li:** Writing – review & editing, Writing – original draft, Visualization, Validation, Methodology, Investigation, Data curation, Conceptualization.

Declaration of competing interest

The authors declare that they have no known competing financial interests or personal relationships that could have appeared to influence the work reported in this paper.

Acknowledgments

This research was funded by the Central Public-interest Scientific Institution Basal Research Fund (CAFYBB2025ZA001), Key Science and Technology Projects of Inner Mongolia Autonomous Region (2024JBGS0019), and Guizhou Education University Scientific Research Fund Project (2024YB002; 2024BSKQ003).

Appendix A. Supplementary data

Supplementary data to this article can be found online at https://doi.org/10.1016/j.indic.2026.101263.

Data availability

Data will be made available on request.

References

Allouche, O., Tsoar, A., Kadmon, R., 2006. Assessing the accuracy of species distribution models: prevalence, kappa and the true skill statistic (TSS). J. Appl. Ecol. 43, 1223–1232. https://doi.org/10.1111/j.1365-2664.2006.01214.x.

Anderson, R.P., Gonzalez, I., 2011. Species-specific tuning increases robustness to sampling bias in models of species distributions: an implementation with maxent. Ecol. Model. 222, 2796–2811. https://doi.org/10.1016/j.ecolmodel.2011.04.011.

Bowler, D.E., Hof, C., Haase, P., Kröncke, I., Schweiger, O., Adrian, R., Baert, L., Bauer, H.-G., Blick, T., Brooker, R.W., Dekoninck, W., Domisch, S., Eckmann, R., Hendrickx, F., Hickler, T., Klotz, S., Kraberg, A., Kühn, I., Matesanz, S., Meschede, A., Neumann, H., O'Hara, R., Russell, D.J., Sell, A.F., Sonnewald, M., Stoll, S., Sundermann, A., Tackenberg, O., Türkay, M., Valladares, F., van Herk, K., van Klink, R., Vermeulen, R., Voigtländer, K., Wagner, R., Welk, E., Wiemers, M., Wiltshire, K.H., Böhning-Gaese, K., 2017. Cross-realm assessment of climate change impacts on species' abundance trends. Nat. Ecol. Evol. 1, 67. https://doi.org/10.1038/s41559-016-0067.

Burnham, K.P., Anderson, D.R., 2004. Multimodel inference: understanding AIC and BIC in model selection. Socio. Methods Res. 33, 261–304. https://doi.org/10.1177/0049124104268644.

Capera-Aragones, P., Tyson, R.C., Foxall, E., 2023. The maximum entropy principle to predict forager spatial distributions: an alternate perspective for movement ecology. Theor. Ecol. 16, 21–34. https://doi.org/10.1007/s12080-023-00552-6.

Chen, J., Hao, W., Shi, Y., Chen, L., Li, H., Zhao, Z., Mo, M., Li, T., 2025. Phytomanagement with forage grasses for sustainable remediation of contaminated tailings soil: enhancing soil functionality and addressing forage safety risks. Environ. Technol. Innov. 40, 104443. https://doi.org/10.1016/j.eti.2025.104443.

Clemente-Villalba, J., Burló, F., Hernández, F., Carbonell-Barrachina, Á.A., 2023. Valorization of wild edible plants as food ingredients and their economic value. Foods 12, 1012. https://doi.org/10.3390/foods12051012.

Cui, G., Zhang, L., Yang, L., A, L., Ren, Z., Ale, R., Ma, P., Sun, J., Liang, E., Pugnaire, F.I., 2025. Caragana versicolor shrub expansion is enhanced by moderate warming but later constrained by climate extremes in the southwestern Tibetan Plateau. Glob. Ecol. Conserv. 59, e03566. https://doi.org/10.1016/j.gecco.2025.e03566.

Deng, L., Yuan, H., Xie, J., Ge, L., Chen, Y., 2022. Herbaceous plants are better than woody plants for carbon sequestration. Resour. Conserv. Recycl. 184, 106431. https://doi.org/10.1016/j.resconrec.2022.106431.

Di Marco, M., Venter, O., Possingham, H.P., Watson, J.E.M., 2018. Changes in human footprint drive changes in species extinction risk. Nat. Commun. 9, 4621. https://doi.org/10.1038/s41467-018-07049-5.

Didan, K., 2015. "MODIS/terra vegetation indices monthly L3 global 1km SIN grid V006. Sioux Falls, South Dakota, USA: NASA land processes distributed active archive center. https://doi.org/10.5067/MODIS/MOD13A3.006.

Dobrowski, S.Z., 2011. A climatic basis for microrefugia: the influence of terrain on climate. Glob. Change Biol. 17, 1022–1035. https://doi.org/10.1111/j.1365-2486.2010.02263.x.

Dormann, C.F., Elith, J., Bacher, S., Buchmann, C., Carl, G., Carré, G., Marquéz, J.R.G., Gruber, B., Lafourcade, B., Leitão, P.J., Münkemüller, T., McClean, C., Osborne, P.E., Reineking, B., Schröder, B., Skidmore, A.K., Zurell, D., Lautenbach, S., 2013. Collinearity: a review of methods to deal with it and a simulation study evaluating their performance. Ecography 36, 27–46. https://doi.org/10.1111/j.1600-0587.2012.07348.x.

Elith, J., Leathwick, J.R., 2009. Species distribution models: ecological explanation and prediction across space and time. Annu. Rev. Ecol. Evol. Systemat. 40, 677–697. https://doi.org/10.1146/annurev.ecolsys.110308.120159.

Franklin, J., 2023. Species distribution modelling supports the study of past, present and future biogeographies. J. Biogeogr. 50, 1533–1545. https://doi.org/10.1111/jbi.14617.

Garcia, R.A., Cabeza, M., Rahbek, C., Araújo, M.B., 2014. Multiple dimensions of climate change and their implications for biodiversity. Science 344, 1247579. https://doi.org/10.1126/science.1247579.

Hallgren, W., Santana, F., Low-Choy, S., Zhao, Y., Mackey, B., 2019. Species distribution models can be highly sensitive to algorithm configuration. Ecol. Model. 408, 108719. https://doi.org/10.1016/j.ecolmodel.2019.108719.

He, K.S., Zhang, J., Zhang, Q., 2009. Linking variability in species composition and MODIS NDVI based on beta diversity measurements. Acta Oecol. 35, 14–21. https://doi.org/10.1016/j.actao.2008.07.006.

Jin, H., Qiao, L., Wang, S., Kong, L., Zhang, J., 2024. Performance evaluation of surface air temperature simulated by the Beijing climate central climate model based on the climate complexity. Clim. Dyn. 62, 4331–4342. https://doi.org/10.1007/s00382-024-07137-x.

Kass, J.M., Muscarella, R., Galante, P.J., Bohl, C.L., Pinilla-Buitrago, G.E., Boria, R.A., Soley-Guardia, M., Anderson, R.P., 2021. ENMeval 2.0: redesigned for customizable and reproducible modeling of species' niches and distributions. Methods Ecol. Evol. 12, 1602–1608. https://doi.org/10.1111/2041-210X.13628.

Keppel, G., Van Niel, K.P., Wardell-Johnson, G.W., Yates, C.J., Byrne, M., Mucina, L., Schut, A.G.T., Hopper, S.D., Franklin, S.E., 2012. Refugia: identifying and understanding safe havens for biodiversity under climate change. Global Ecol. Biogeogr. 21, 393–404. https://doi.org/10.1111/j.1466-8238.2011.00686.x.

Landis, J.R., Koch, G.G., 1977. The measurement of observer agreement for categorical data. Biometrics 33, 159–174. https://doi.org/10.2307/2529310.

Lenoir, J., Hattab, T., Pierre, G., 2017. Climatic microrefugia under anthropogenic climate change: implications for species redistribution. Ecography 40, 253–266. https://doi.org/10.1111/ecog.02788.

Lesk, C., Anderson, W., Rigden, A., Coast, O., Jägermeyr, J., McDermid, S., Davis, K.F., Konar, M., 2022. Compound heat and moisture extreme impacts on global crop yields under climate change. Nat. Rev. Earth Environ. 3, 872–889. https://doi.org/10.1038/s43017-022-00368-8.

Lesk, C., Rowhani, P., Ramankutty, N., 2016. Influence of extreme weather disasters on global crop production. Nature 529, 84–87. https://doi.org/10.1038/nature16467.

Li, Y., Li, M., Li, C., Liu, Z., 2020. Optimized maxent model predictions of climate change impacts on the suitable distribution of *Cunninghamia lanceolata* in China. Forests 11, 302. https://doi.org/10.3390/f11030302.

Liao, D., Zhou, B., Xiao, H., Zhang, Y., Zhang, S., Su, Q., Yan, X., 2025. MaxEnt modeling of the impacts of human activities and climate change on the potential distribution of *plantago* in China. Biology 14, 564. https://doi.org/10.3390/biology14050564.

Liao, H., Kao, W., 2023. Coordination of leaf photosynthetic traits and chloroplast relocation of the C4 plant *Setaria palmifolia*. Flora 306, 152365. https://doi.org/10.1016/j.flora.2023.152365.

Liu, Q., Zhang, H., He, M., Shi, J., Ma, Y., 2025. Potential habitat suitability analysis under climate change for the native grass, *Kengyilia thoroldiana*, on the Qinghai–Tibet Plateau. Agronomy 15. https://doi.org/10.3390/agronomy15020481.

Mechergui, K., Hayat, U., Ahmad, M.H., Alamri, S.M., Alamery, E.R., Faqeih, K.Y., Aldubehi, M.A., Jaouadi, W., 2025. Forecasting the impact of climate change on *Tetraclinis articulata* distribution in the mediterranean using MaxEnt and GIS-based analysis. Forests 16, 1600. https://doi.org/10.3390/f16101600.

Mu, H., Li, X., Wen, Y., Huang, J., Du, P., Su, W., Miao, S., Geng, M., 2022. A global record of annual terrestrial human footprint dataset from 2000 to 2018. Sci. Data 9, 176. https://doi.org/10.1038/s41597-022-01284-8.

Muscarella, R., Galante, P.J., Soley-Guardia, M., Boria, R.A., Kass, J.M., Uriarte, M., Anderson, R.P., 2014. ENMeval: an R package for conducting spatially independent evaluations and estimating optimal model complexity for maxent ecological niche models. Methods Ecol. Evol. 5, 1198–1205. https://doi.org/10.1111/2041-210X.12261.

Naimi, B., 2015. "usdm: uncertainty analysis for species distribution models. R Package Version 2.1-7, R Documentation. https://rdocumentation.org/packages/usdm/versions/2.1-7.

Nan, Z., 2005. The grassland farming system and sustainable agricultural development in China. Grassl. Sci. 51, 15–19. https://doi.org/10.1111/j.1744-697X.2005.00003.x.

Parmesan, C., Yohe, G., 2003. A globally coherent fingerprint of climate change impacts across natural systems. Nature 421, 37–42. https://doi.org/10.1038/nature01286.

Pearson, R.G., Dawson, T.P., 2003. Predicting the impacts of climate change on the distribution of species: are bioclimate envelope models useful? Global Ecol. Biogeogr. 12, 361–371. https://doi.org/10.1046/j.1466-822X.2003.00042.x.

Phillips, S.J., Dudík, M., 2008. Modeling of species distributions with maxent: new extensions and a comprehensive evaluation. Ecography 31, 161–175. https://doi.org/10.1111/j.0906-7590.2008.5203.x.

Roberts, D.R., Bahn, V., Ciuti, S., Boyce, M.S., Elith, J., Guillera-Arroita, G., Hauenstein, S., Lahoz-Monfort, J.J., Schröder, B., Thuiller, W., Warton, D.I., Wintle, B.A., Hartig, F., Dormann, C.F., 2017. Cross-validation strategies for data with temporal, spatial, hierarchical, or phylogenetic structure. Ecography 40, 913–929. https://doi.org/10.1111/ecog.02881.

Román-Palacios, C., Wiens, J.J., 2020. Recent responses to climate change reveal the drivers of species extinction and survival. Proc. Natl. Acad. Sci. 117, 4211–4217. https://doi.org/10.1073/pnas.1913007117.

Soberón, J., Nakamura, M., 2009. Niches and distributional areas: concepts, methods, and assumptions. Proc. Natl. Acad. Sci. 106, 19644–19650. https://doi.org/10.1073/pnas.0901637106.

Tatian, M., Borna, F., Gholami, V., Faraji, A., 2025. Predicting habitat destruction of rangeland plant species using the maximum entropy algorithm (MaxEnt) and geographic information system (GIS). Plant Ecol. 226, 721–733. https://doi.org/10.1007/s11258-025-01523-z.

Tian, Z., Wang, J.-W., Li, J., Han, B., 2021. Designing future crops: challenges and strategies for sustainable agriculture. Plant J. 105, 1165–1178. https://doi.org/10.1111/tpj.15107.

Veloz, S.D., 2009. Spatially autocorrelated sampling falsely inflates measures of accuracy for presence-only niche models. J. Biogeogr. 36, 2290–2299. https://doi.org/10.1111/j.1365-2699.2009.02174.x.

Warren, D.L., Seifert, S.N., 2011. Ecological niche modeling in maxent: the importance of model complexity and the performance of model selection criteria. Ecol. Appl. 21, 335–342. https://doi.org/10.1890/10-1171.1.

Williams, J.W., Jackson, S.T., 2007. Novel climates, No-Analog communities, and ecological surprises. Front. Ecol. Environ. 5, 475–482. https://doi.org/10.1890/070037.

Wu, Z., Hou, X., Ren, W., Wang, Z., Chang, C., Yang, Y., Yang, Y., 2018. Prediction of the potential geographic distribution of *Leymus chinensis* based on MaxEnt and collection and protection of germplasm. Acta Prataculturae Sinica 27, 125–135. https://doi.org/10.11686/cyxb2018052 (In Chinese with English Abstract).

Xiang, Y., Li, S., Yang, Q., Ren, J., Liu, Y., Luo, Y., Zhao, L., Luo, X., Yao, B., Guo, X., 2025. Forecasting northward range expansion of switchgrass in China via multi-Scenario MaxEnt simulations. Biology 14, 1061. https://doi.org/10.3390/biology14081061.

Xin, X., Wu, T., Zhang, J., Yao, J., Fang, Y., 2020. Comparison of CMIP6 and CMIP5 simulations of precipitation in China and the East Asian summer monsoon. Int. J. Climatol. 40, 6423–6440. https://doi.org/10.1002/joc.6590.

Xing, Y., Shi, J., De, K., Wang, X., Wang, W., Ma, Y., Zhang, H., He, M., Liu, Q., 2023. The current distribution of *Carex alatauensis* in the Qinghai–Tibet Plateau estimated by MaxEnt. Agronomy 13. https://doi.org/10.3390/agronomy13020564.

Xu, C., Zhang, L., Zhang, K., Tao, J., 2023a. MaxEnt modeling and the impact of climate change on *Pistacia chinensis* bunge habitat suitability variations in China. Forests 14. https://doi.org/10.3390/f14081579.

Xu, Y., Zhu, R., Gao, L., Huang, D., Fan, Y., Liu, C., Chen, J., 2023b. Predicting the current and future distributions of *Pennisetum alopecuroides* (L.) in China under climate change based on the MaxEnt model. PLoS One 18, e0281254. https://doi.org/10.1371/journal.pone.0281254.

Yan, X., Wang, S., Duan, Y., Han, J., Huang, D., Zhou, J., 2021. Current and future distribution of the deciduous shrub *Hydrangea macrophylla* in China estimated by MaxEnt. Ecol. Evol. 11, 16099–16112. https://doi.org/10.1002/ece3.8288.

Yang, Y., Tilman, D., Jin, Z., Smith, P., Barrett, C.B., Zhu, Y.-G., Burney, J., D'Odorico, P., Fantke, P., Fargione, J., Finlay, J.C., Rulli, M.C., Sloat, L., Jan van Groenigen, K., West, P.C., Ziska, L., Michalak, A.M., the Clim-Ag, T., Lobell, D.B., Clark, M., Colquhoun, J., Garg, T., Garrett, K.A., Geels, C., Hernandez, R.R., Herrero, M., Hutchison, W.D., Jain, M., Jungers, J.M., Liu, B., Mueller, N.D., Ortiz-Bobea, A., Schewe, J., Song, J., Verheyen, J., Vitousek, P., Wada, Y., Xia, L., Zhang, X., Zhuang, M., 2024. Climate change exacerbates the environmental impacts of agriculture. Science 385, eadn3747. https://doi.org/10.1126/science.adn3747.

Yang, Z., Solangi, Y.A., 2024. Analyzing the relationship between natural resource management, environmental protection, and agricultural economics for sustainable development in China. J. Clean. Prod. 450, 141862. https://doi.org/10.1016/j.jclepro.2024.141862.

Zhang, K., Lin, J., Zheng, J., Li, X., Xu, L., Liu, L., Liu, X., Jin, X., Fu, R., Wang, X., Sang, Y., Guo, X., 2025. Evaluating climate change effects on swan habitats within China: adaptive strategies for sustainable conservation. Ecol. Evol. 15, e72238. https://doi.org/10.1002/ece3.72238.

Zhang, X., Liu, T., Ren, S., Liu, S., Lin, C., Ji, B., 2023. Identification of potential areas of three wild forages in Tibet region based on MaxEnt model. Acta Agrestia Sinica 31, 2314–2322. https://doi.org/10.11733/i.issn.1007-0435.2023.08.007 (In Chinese with English Abstract).

Zhao, S., Zhang, Z., Gao, C., Dong, Y., Jing, Z., Du, L., Hou, X., 2025a. MaxEnt-Based predictions of suitable potential distribution of *Leymus secalinus* under current and future climate change. Plants 14. https://doi.org/10.3390/plants14020293.

Zhao, W., Suo, L., Wang, T., Wang, Y., Fan, L., Luo, T., Wang, X., Yang, L., Zhang, L., 2025b. Climate change is leading to geographic expansion of tropical birds—range expansion and niche modeling in the White-browed crake (*Pololimnas cinereus*). BMC Ecol. Evol. 25, 138. https://doi.org/10.1186/s12862-025-02455-y.

Zhu, K., Woodall, C.W., Clark, J.S., 2012. Failure to migrate: lack of tree range expansion in response to climate change. Glob. Change Biol. 18, 1042–1052. https://doi.org/10.1111/j.1365-2486.2011.02571.x.